Pramāṇa, Vol. 16, No 5, May 1981, pp. 391–402. © Printed in India.

Optical reaction cross-sections for light projectiles

A CHATTERJEE, K H N MURTHY* and S K GUPTA
Nuclear Physics Division, Bhabha Atomic Research Centre, Bombay 400 085, India
*Department of Physics, University of Mysore, Mysore 570 006, India

MS received 1 October 1980; revised 6 March 1981

Abstract. The optical reaction cross-sections for *n*, *p*, ^{2}H, ^{3}H, ^{3}He and ^{4}He for several global optical potentials available in the literature have been parametrized in terms of simple empirical expressions which are smooth functions of the target mass number and the projectile energy. The empirical forms are 5–10% accurate over the periodic table and energy-range upto 50 MeV. They can be conveniently used in calculations where the optical reaction cross-sections are required as input. The calculation of proton spectra in the (*n*, *p*) reaction at 14 MeV is discussed.

Keywords. Optical reaction cross-sections; empirical parametrization; evaporation; preequilibrium models; light projectiles; parametric forms; neutrons; charged particles.

1. Introduction

The non-elastic part of the interaction between the incident particle and the target nucleus manifests itself as the reaction cross-section. As a first approximation this interaction is described by a complex (optical) potential, the imaginary part of which leads to a finite reaction cross-section. In the literature the projectile-target interaction for target nuclei over the periodic chart has been given in terms of global optical parameter-sets. The reaction cross-sections generated using these global parameters are employed in several further calculations. In the statistical evaporation theory and the preequilibrium model the break-up of the total reaction cross-section into partial modes involving the emission of one or more particles is described by emission rate expressions which contain the cross-sections for the inverse processes involving the emitted particle as a function of energy. The cross-section for the inverse process is the optical reaction cross-section of the excited residual nucleus with the emitted particle as the projectile. This is approximated as the optical reaction cross-section between the residual nucleus in its ground state and the (emitted) particle. Thus optical reaction cross-sections are required for the incident channel at the projectile energy and for the exit channels over the energy range of the emitted particles. The statistical evaporation theory is a widely-used description for reactions at low energies. At energies in the range of several tens of MeV the preequilibrium models have been successful. Reaction cross-sections are also used in intra-nuclear-cascade calculations (Kikuchi and Kawai 1968) and in the calculation of the nuclear-reaction efficiency correction for detectors (Makino *et al* 1968).

Usually the optical reaction cross-sections at all the required energies and particle-target combinations are obtained by a numerical solution of the Schrödinger equation for several partial waves. This involves a large amount of computation time. Also, where more than one global optical potential appears in the literature for the same projectile it is quite laborious to repeat the calculations for each of the sets to see the effect on the final results.

In this work the optical reaction cross-sections for n, p, ^2H, ^3H, ^3He and ^4He are directly parametrized in a simple form. The parametrization predicts the optical reaction cross-sections for nuclei over the periodic table and energies upto 50 MeV. In the energy space these empirical forms are simple polynomials and consequently the emission-rate expressions (using simple forms for the level density) are integrable over the spectrum of final states in a closed form. This work can be considered as a major improvement over an earlier parametrization (Dostrovsky *et al* 1959) where the continuum model cross-sections (Blatt and Weisskopf 1952; Shapiro 1953) were the input. A preliminary report of the present work has been given earlier (Chatterjee and Gupta 1978b, Murthy *et al* 1979a, b).

In §2 the global optical model potentials considered in this work are discussed. The parametric forms which describe the reaction cross-section generated by these potentials are described in §3. The parametrization of Dostrovsky *et al* (1959) is also compared. The application of the empirical expressions in statistical model calculations is discussed in §4.

2. Optical model potential

The form of the optical potential is (Perey and Perey 1974),

$$U(r, E) = -U_N(r, E) + V_c(r) + U_{\text{so}}(r), \tag{1}$$

where V_c is the Coulomb potential due to a uniformly-charged sphere with radius r_c, U_{so} is the spin-orbit potential and U_N is the complex central potential taken as,

$$U_N(r, E) = V_R(E) f(x_R) + i\,[W_V(E) f(x_V) + W_S(E) g(x_S)], \tag{2}$$

where $f(x_R) = [1 + \exp(x_R)]^{-1}$ with $x_R = (r - r_R A^{1/3})/a_R$

$$g(x_S) = -4 \frac{d}{dx_S} f(x_S) \text{ (Woods-Saxon derivative)}$$

$$\text{or } \exp(-x_S^2) \text{ (Gaussian).}$$

Here x_V and x_S are defined in the same manner with appropriate radius parameters r_S, r_V and diffuseness paramers a_S, a_V. The spin-orbit potential U_{so} is, given by,

$$U_{\text{so}}(r) = \lambda_\pi^2 (\mathbf{l} \cdot \sigma) \frac{1}{r} \frac{d}{dr} f(x_{\text{so}}) V_{\text{so}}. \tag{3}$$

Using this form of the potential several extensive analyses of differential elastic, polarization and reaction cross-section data have been carried out by various workers resulting in global parameter sets. For neutrons the global set of Wilmore and Hodgson (1964) can be considered to be the most useful one. This is the local equivalent version of the non-local potential of Perey and Buck (1962). The potential of Becchetti and Greenless (1969) both for protons and neutrons are also well-known. We have also included the optical potentials of Mani *et al* (1963) both for protons and neutrons since the tables using these sets are often used. For protons the parameter-sets of Perey (1963) and Menet *et al* (1971) are also considered. For other projectiles the parameter-sets used are those of Lohr and Haeberli (1974) and Schwandt and Haeberli (1969) for deuterons; and Becchetti and Greenlees (1971) for ^{3}H and ^{3}He. For alpha particles there does not exist a clear-cut global phenomenological parameter set. Here the cross-sections listed in Huizenga and Igo's (1961) table were used directly in fitting the parametric forms.

3. Parametric forms for the reaction cross-section

Using the global optical potential parameters described above, the code SCAT (Smith 1969) was used to generate the reaction cross-sections for the projectiles *n*, *p*, ^{2}H, ^{3}H and ^{3}He from 1-50 MeV for 23 nuclei in the mass range 20-214. For ^{4}He the reaction cross-sections over an energy range 2-46 MeV and mass range 20-206 were taken from the existing tabulation (Huizenga and Igo 1961). The parameters of the empirical forms were determined by a fit to these cross-sections.

3.1 *Neutrons*

For energy dependence in the case of neutrons the optical reaction cross-section σ_R (in millibarns) is written as,

$$\sigma_R = \lambda\epsilon + \mu + \nu/\epsilon, \tag{4}$$

where λ, μ, ν are mass-dependent parameters and ϵ is the neutron laboratory energy in MeV. The addition of the linear term $\lambda\epsilon$ greatly improves the fit as compared to the parametric form of Dostrovsky *et al* (1959). Separating out the energy dependence as in (4), the dependence of λ, μ, ν on target mass number A, was obtained empirically as,

$$\lambda = \lambda_0 A^{-1/3} + \lambda_1$$

$$\mu = \mu_0 A^{1/3} + \mu_1 A^{2/3},$$

$$\nu = \nu_0 A^{4/3} + \nu_1 A^{2/3} + \nu_2. \tag{5}$$

The seven parameters λ_0 through ν_2 were determined by a linear-least-squares fit of σ_R and are given in table 1. A comparison of the σ_R predicted by the empirical parametrization and that generated from the global optical potentials for neutrons is shown in figure 1.

Table 1. Parameters determined by a fit to various reaction cross sections.

	p_0	p_1	p_2	λ_0	λ_1	μ_0	μ_1	ν_0	ν_1	ν_2
Neutrons										
Mani *et al* (1963)	—	—	—	15·30	−14·98	297·7	30·58	0·320	−47·08	74·19
Becchetti and Greenlees (1969)	—	—	—	18·57	−22·93	381·7	24·31	0·172	−15·39	804·8
Wilmore and Hodgson (1964)	—	—	—	31·05	−25·91	342·4	21·89	0·223	0·673	617·4
Continuum	—	—	—	0	0	155·5	53·72	0	−3·534	156·9
Protons										
Mani *et al* (1963)	12·97	15·65	−348·5	0·0247	−7·01	300·4	0·40	330·0	−223·6	−3·251
Perey (1963)	10·53	52·53	−414·0	0·0310	−10·16	327·9	0·40	323·7	−243·4	−3·037
Becchetti and Greenlees (1969)	15·72	9·65	−449·0	0·00437	−16·58	244·7	0·503	273·1	−182·4	−1·872
Menet *et al* (1971)	16·99	46·13	−1298	−0·0795	−11·90	127·8	0·66	306·8	−118·5	0·225
Continuum	—	—	—	0	0	135·8	0·56	215·9	−115·2	−0·875
Deuterons										
Schwandt and Haeberli (1969)	−43·73	934·1	−2518	−0·0761	−8·83	337·5	0·49	417·5	−353·0	5·515
Lohr and Haeberli (1974)	−38·21	922·6	−2804	−0·0323	−5·48	336·1	0·48	524·3	−371·8	−5·924
Continuum	—	—	—	0	0	230·0	0·50	257·4	−198·2	−2·150
Tritons										
Becchetti and Greenlees (1971)	−11·04	619·1	−2147	−0·0426	−10·33	601·9	0·37	583·0	−546·2	1·718
Continuum		—	—	—	0	0	203·9	0·52	262·5	−206·50
He-3										
Becchetti and Greenlees (1971)	−3·06	278·5	−1389	−0·00535	−11·16	555·5	0·40	687·4	−476·3	0·509
Continuum	—	—	—	0	0	203·1	0·53	448·6	−207·9	0
He-4										
Huizenga and Igo (1961)	10·95	−85·2	1146	0·0643	−13·96	781·2	0·29	−304·7	−470·0	−8·580
Continuum	—	—	—	0	0	189·2	0·54	408·5	−204·5	0

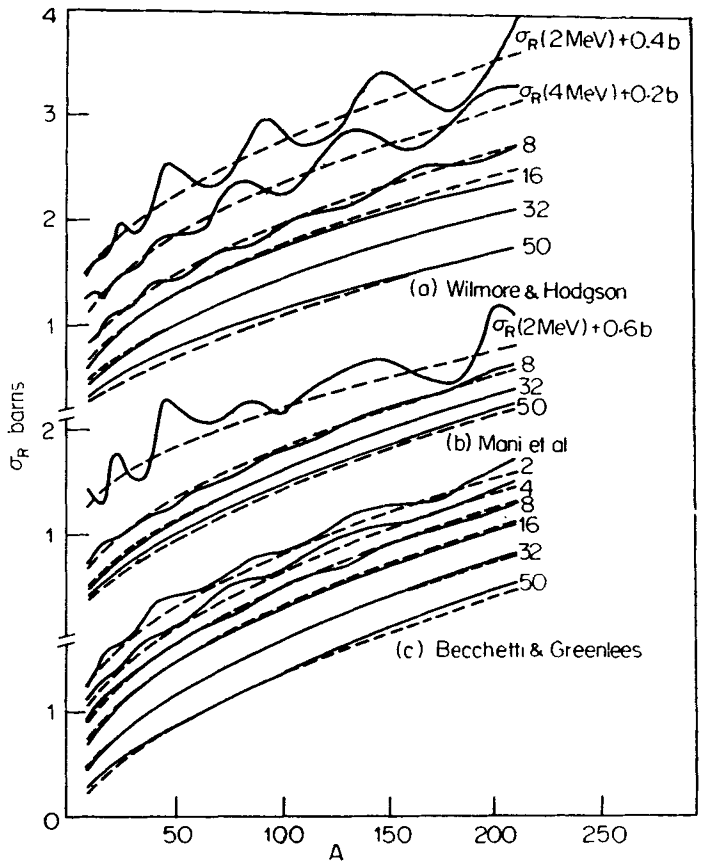

Figure 1. Comparison of the neutron optical reaction cross-sections (solid curve) with the predictions of the empirical formula (dotted curve) as a function of the target mass A for the global potentials of (a) Wilmore and Hodgson (1964) (b) Mani *et al* (1963) and (c) Becchetti and Greenlees (1969). The numbers to the right of the curves indicate the lab. energy in MeV. For the sake of clarity some of the curves have been displaced as indicated.

3.2 *Charged particles*

For charged particles an adequate description of the energy dependence of σ_R and particularly the rapid fall below the Coulomb barrier was obtained by using an energy dependence as in (4) above the Coulomb barrier, E_c and a quadratic energy dependence,

$$\sigma_R = p\epsilon^2 + q\epsilon + r \quad \text{(mb)}, \tag{6}$$

for $\epsilon < E_c$. Here E_c is taken as,

$$E_c = 1{\cdot}44\, zZ/(1{\cdot}5\, A^{1/3} + \delta) \quad \text{(MeV)}, \tag{7}$$

where z and Z are the charge numbers of the projectile and target respectively and $\delta = 0$ for protons and 1·2 for the other charged projectiles. Matching expressions (4) and (6) for their value and derivative at $\epsilon = E_c$, q and r can be eliminated,

$$q = \lambda - \nu/E_c^2 - 2\,p\,E_c,$$

$$r = \mu + 2\,\nu/E_c + p\,E_c^2, \tag{8}$$

and σ_R is expressed over the full energy domain as,

$$\sigma_R = p\,(\epsilon - \xi)^2 + \lambda\epsilon + \mu + \nu\,(2 - \epsilon/\xi)/\xi, \tag{9}$$

where

$$\xi = \max\,(\epsilon, E_c).$$

Here the parameters p and ν play a dominant role in the description of σ_R below the Coulomb barrier and were parametrized in terms of E_c. The other parameters λ and μ were parametrized in terms of the target mass number A. The following parametrization was found successful,

$$p = p_0 + p_1/E_c + p_2/E_c^2,$$

$$\lambda = \lambda_0\,A + \lambda_1,$$

$$\mu = \mu_0\,A^{\mu_1},$$

$$\nu = A^{\mu_1}\,[\nu_0 + \nu_1\,E_c + \nu_2\,E_c^2]. \tag{10}$$

The parameters p_0 through ν_2 were determined by a least squares fit to the optical cross-sections σ_R for various global parameter sets for the projectiles, p, ^{2}H, ^{3}H, ^{3}He and ^{4}He. In the fitting process μ_1 is the only non-linear parameter. Its value was obtained by a search in small steps while the other parameters were determined by a linear-least-squares code. Using these 10 parameters the mass number and energy dependence of σ_R is adequately described. The success of the parametrization is illustrated in figures 2 and 3. The values of the parameters for all these projectiles and various optical potential parameter sets are given in table 1.

Equation (9) predicts unphysical or negative values of σ_R over a small domain $0 < \epsilon < E_0$. In using (9), σ_R should be set to zero in this domain. The energy E_0 can be determined from the roots ϵ_1, ϵ_2 of the quadratic equation, $p\epsilon^2 + q\epsilon + r = 0$, as,

$$E_0 = \max\,(\epsilon_1, \epsilon_2) \qquad (p > 0),$$

$$= \min\,(\epsilon_1, \epsilon_2) \qquad (p < 0), \tag{11}$$

where E_0 is zero when expression (11) is negative.

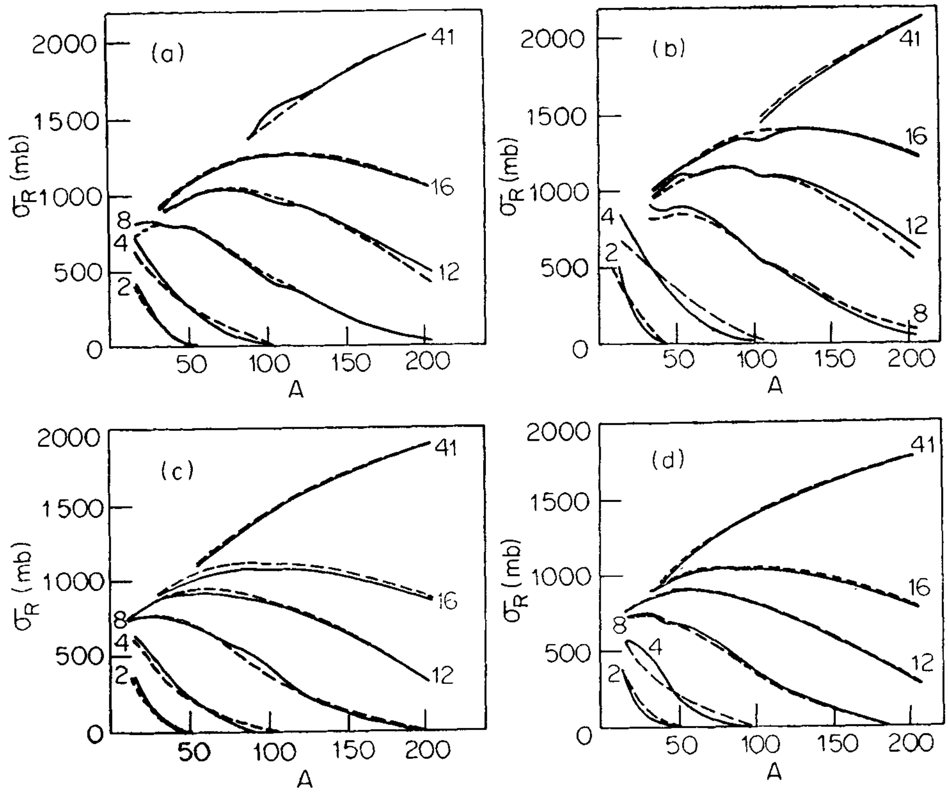

Figure 2. Comparison of the proton optical reaction cross-sections (solid curve) with the predictions of the empirical formula (dotted curve) as a function of the target mass A for the global potentials of (**a**) Becchetti and Greenlees (1969) (**b**) Menet *et al* (1971) (**c**) Perey (1963) and (**d**) Mani *et al* (1963). The numbers on the curves indicate the lab. energy in MeV.

3.3 *Comparison with the earlier parametrization*

The parametrization of Dostrovsky *et al* (1959) is similar to (4) but does not include the linear term in ϵ for neutrons as well as for charged particles. Their parameters were determined by a fit to the continuum model cross-sections. The continuum model corresponds to an optical model which has an infinitely absorbing square-well potential. The parameters of the optical model incorporating a finitely absorbing diffuse potential, are obtained from the analysis of a large amount of scattering data and are therefore more realistic than the continuum model.

The parameters of Dostrovsky *et al* (1959) for neutrons are included in table 1. For charged particles their parameters are given for 5 nuclei. In order to facilitate a comparison, we have re-cast these parameters to have A and Z dependence similar to (10) listing the results in table 1. In this case $\sigma_R = \mu + \nu/\epsilon$ is to be used for $\epsilon < E_c$ as well.

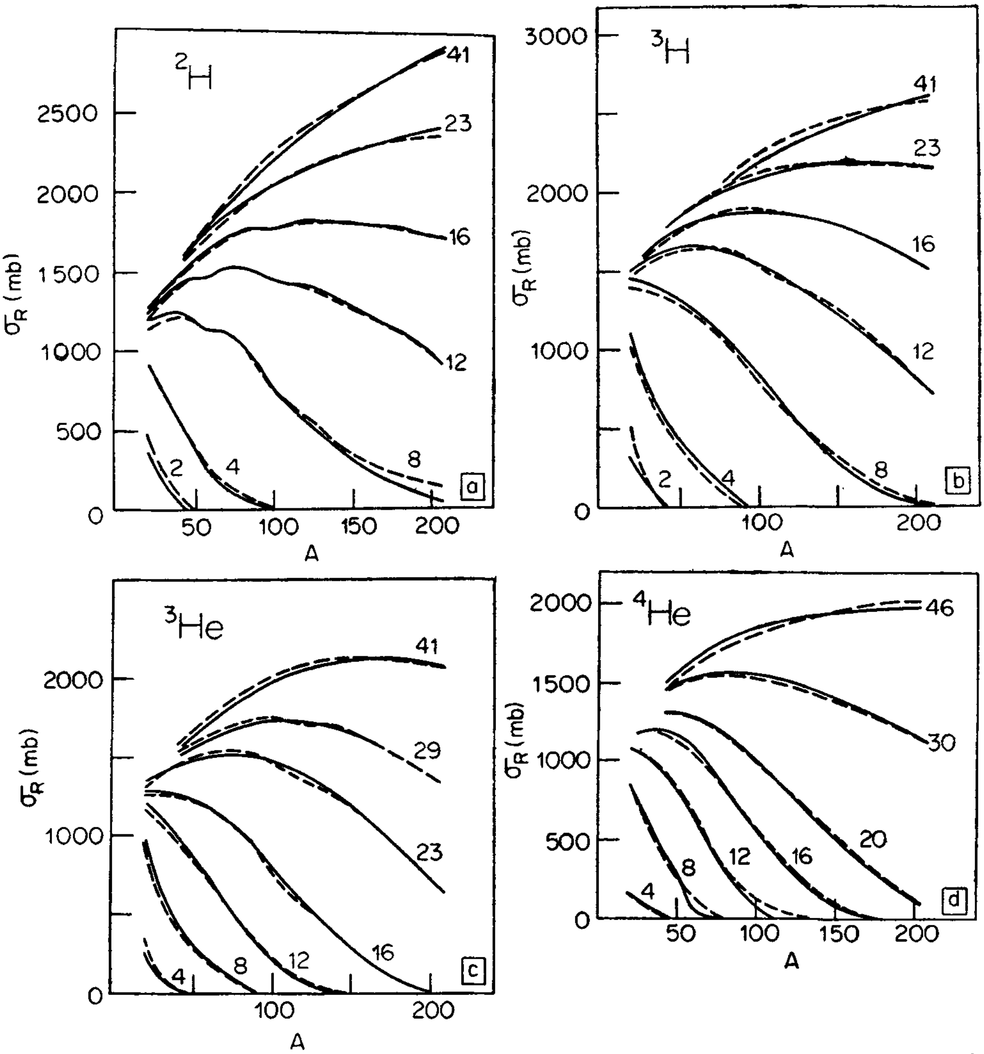

Figures 3a-d. Same as Figure 2 for ^{2}H, ^{3}H, ^{3}He and ^{4}He, for the global potentials of Schwandt-Haeberli (1969) for ^{2}H, Becchetti-Greenlees (1971) for ^{3}H and ^{3}He and the optical cross sections of Huizenga-Igo for ^{4}He.

A detailed comparison of the Dostrovsky cross-sections (σ_D) and the cross-section ($\sigma_{\rm fit}$) of the present parametrization is exemplified in figure 4 by plotting $\sigma_D/\sigma_{\rm fit}$ as a function of projectile energy for ^{45}Sc. The $\sigma_{\rm fit}$ values correspond to the optical potentials of Wilmore-Hodgson (1964) for neutrons, Becchetti-Greenlees (1969) for protons, Schwandt-Haeberli (1969) for deuterons, Becchetti-Greenlees (1971) for ^{3}H and ^{3}He and the cross-sections of Huizenga-Igo (1961) for ^{4}He. The combined parametrization of (4) and (6) gives a better fit to the sub-Coulomb cross-sections for charged particles, while σ_D goes to zero at about 0·6 E_C for protons and deuterons, 0·7 E_C for ^{3}H and ^{3}He and 0·8 E_C for ^{4}He. For $\epsilon > 10$ MeV, $\sigma_D/\sigma_{\rm fit}$ varies from 0·6 to 1·5 for the charged particles. For neutrons $\sigma_D/\sigma_{\rm fit}$ varies from 0·5 to 1·9. A qualitatively similar behaviour is observed for other targets as well.

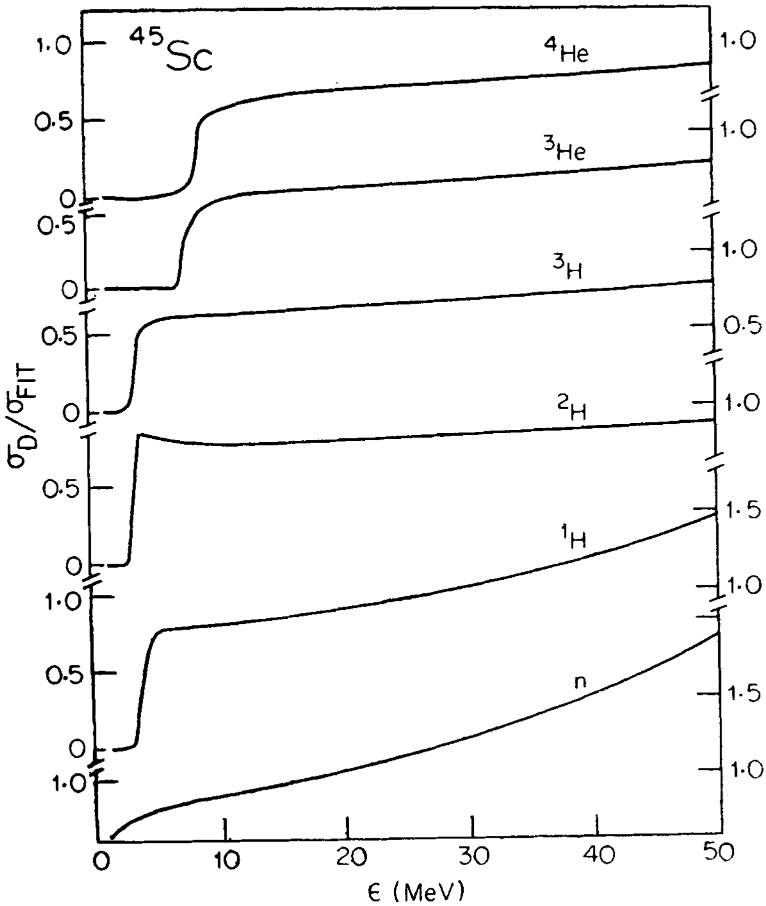

Figure 4. Ratio $\sigma_D/\sigma_{\text{fit}}$ of the parametrized reaction cross sections σ_D of Dostrovsky *et al* (1959) and σ_{fit} of the present work for ^{45}Sc as a function of projectile energy.

4. Applications

In both the statistical evaporation (Weisskopf 1937) and the preequilibrium (Blann 1975) models the differential emission rate for a particle x is,

$$dW_x/d\epsilon = C(x, E^*)\, \epsilon\, \sigma_x(\epsilon)\, \rho\, (E - \epsilon)\, d\epsilon, \qquad (12)$$

where $C(x, E^*)$ is a constant depending upon x and the composite system excitation energy E^*; $E = E^* - S_x$, where S_x is the binding energy of the particle; ρ is the level-density of the residual system; and σ_x is the optical reaction cross-section of x with the residual nucleus. From (12) the preequilibrium proton spectra for the (n, p) reaction at 14 MeV (figure 5) were calculated by Braga-Marcazzan *et al* (1972) using the optical cross-sections of Mani *et al* (1963). On repeating the calculation using the present parametrization of these cross-sections the predicted spectra are nearly identical, while the spectra calculated using the parametrization of

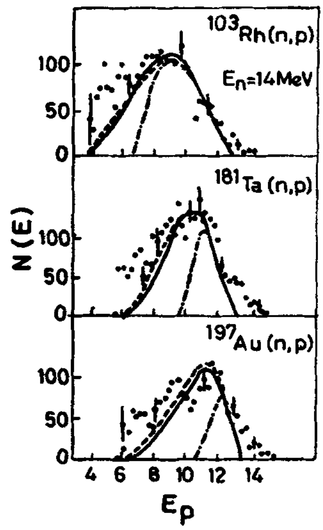

Figure 5. Proton spectra for the (n, p) reaction at 14 MeV. The solid line and experimental points are from Braga-Marcazzan *et al* (1972). The dashed and dot-dashed curves are calculated using the present parametrization and that of Dostrovsky *et al* (1959) respectively. The ordinate is in arbitrary units.

Dostrovsky *et al* (1959) differ considerably. This establishes the importance of the present parametrization.

Using the parametric forms (4) and (6) the emission rates,

$$W_x = \int_0^E (dW_x/d\epsilon)\, d\epsilon$$

can be expressed in a closed form. For the evaporation theory with a level-density (Bethe 1937),

$$\rho(E) = \rho_0 \exp\left(2\sqrt{aE}\right), \tag{13}$$

the emission rate is,

$$W = \frac{C\rho_0}{2a}\left[\sum_{i=0}^{3} \frac{(-)^i}{i!\,(4a)^i} K_i \frac{d^i}{dE^i} F(E) + \sum_{i=0}^{2} \frac{(-)^i}{i!\,(4a)^i} L_i \frac{d^i}{dE^i} G(E)\right], \tag{14}$$

where
$$F(E) = pE^3 + qE^2 + rE,$$

$$G(E) = \lambda E^2 + \mu E + \nu$$

$$K_i = I_i\left\{2\left[a(E-E_0)\right]^{1/2}\right\} - I_i\left\{2\left[a(E-E_c)\right]^{1/2}\right\}$$

$$L_i = I_i\left\{2\left[a(E-E_c)\right]^{1/2}\right\} - I_i(0)$$

$$I_i(x) = -(2i+1)!\, e^x \sum_{r=0}^{2n+1} (-x)^r/r! \tag{15}$$

For the preequilibrium model, the state density (Griffin 1966) of an n-exciton state with p particles and h holes ($n = p+h$) is,

$$\rho(p, h, E) = g^n E^{n-1}/p!\, h!\, (n-1)! \tag{16}$$

The emission rate is,

$$W = \frac{C g^n}{p!\, h!\, (n-1)!} \left[\sum_{i=0}^{3} \frac{(-)^i}{i!} M_i \frac{d^i}{dE^i} F(E) + \sum_{i=0}^{2} \frac{(-)^i}{i!} N_i \frac{d^i}{dE^i} G(E) \right], \tag{17}$$

where

$$M_i = J_i(E - E_0) - J_i(E - E_c),$$

$$N_i = J_i(E - E_c) - J_i(0),$$

$$J_i(x) = x^{i+n}/(i+n). \tag{18}$$

In (14) and (17) both the first sum and E_c are zero for neutron emission.

These results have been employed earlier (Chatterjee and Gupta 1978a, 1979).

5. Discussion

The present parametrization of reaction cross-sections for n, p, ^2H, ^3H, ^3He and ^4He reproduces the optical model values satisfactorily over the mass range 16-214 and energies upto 50 MeV and it is useful for applications. For neutrons the parametric form describes the gross behaviour of σ_R but at low energies does not reproduce its oscillations which are due to the size resonance effect. For $\epsilon > 3$ MeV the accuracy is better than 5% except for the oscillations. For $\epsilon < 2$ MeV the cross-sections are not well reproduced at low mass numbers for the case of Mani *et al* (1963). For protons the size resonance effect is suppressed due to the Coulomb barrier and the parametric form is accurate to 5% except at $\epsilon \sim 4$ MeV, where it is accurate to 10%. However, in this case the cross-sections are small and do not contribute significantly in applications where an integral over a large energy domain is computed. For ^2H, ^3H, ^3He and ^4He the cross-sections are reproduced to better than 5% except for the low values of σ_R in the case of heavy targets at energies well below the Coulomb barrier. The present parametric form cannot be extrapolated far beyond 50 MeV due to the term linear in energy.

Acknowledgements

One of the authors (KHNM) thanks Dr M K Mehta and Prof. B Sanjeevaiah for their encouragement during this work.

References

Becchetti F D and Greenlees G W 1969 *Phys. Rev.* **182** 1190

Becchetti F D and Greenlees G W 1971 *Polarization phenomena in nuclear reactions* (eds H H Barschall and W Haeberli) (Univ. of Wisconsin Press) p. 682

Bethe H A 1937 *Rev. Mod. Phys.* **9** 69

Blann M 1975 *Annu. Rev. Nucl. Sci.* **25** 123

Blatt J and Weisskopf V F 1952 *Theoretical nuclear physics* (New York: John Wiley)

Braga-Marcazzan G M, Gadioli Erba E, Millazo Colli L and Sona P G 1972 *Phys. Rev.* **C6** 1398

Chatterjee A and Gupta S K 1978a *Phys. Rev.* **C18** 2118

Chatterjee A and Gupta S K 1978b *Proc. Nucl. Phys. Solid. State Phys. Symp.* **B21** 118

Chatterjee A and Gupta S K 1979 Int. Conf. on Nucl. Cross Sections for Technology, Knoxville, contributed paper GB10

Dostrovsky I, Fraenkel Z and Friedlander G 1959 *Phys. Rev.* **116** 683

Griffin J J 1966 *Phys. Rev. Lett.* **17** 478

Huizenga J R and Igo G T 1961 Argonne National Laboratory Report No. ANL-6373 (unpublished)

Kikuchi K and Kawai M 1968 *Nuclear matter and nuclear reactions* (Amsterdam: North Holland) p. 262

Lohr J M and Haeberli W 1974 *Nucl. Phys.* **A232** 381

Makino M Q, Waddel C N and Eisberg R M 1968 *Nucl. Inst. Meth.* **60** 109

Mani G S, Melkanoff M A and Iori I 1963 Reports CEA-2379 and—2380 (unpublished)

Menet J J H, Gross E E, Malanify J J and Zucker A 1971 *Phys. Rev.* **C4** 1114

Murthy K H N, Chatterjee A and Gupta S K 1979a *Nucl. Phys. Solid. State Phys. Symp.*, Madras, contributed paper NO4

Murthy K H N, Chatterjee A and Gupta S K 1979b Int. Conf. on Nucl. Cross Section for Technology, Knoxville, contributed paper GB 11

Perey F G 1963 *Phys. Rev.* **131** 145

Perey F G and Buck B 1962 *Nucl. Phys.* **32** 353

Perey C M and Perey F G 1974 *Atomic Nucl. Data Tables* **13** 293

Schwandt P and Haeberli W 1969 *Nucl. Phys.* **A123** 401

Shapiro M M 1953 *Phys. Rev.* **90** 171

Smith W R 1969 *Comp. Phys. Comm.* **1** 106

Weisskopf V F 1937 *Phys. Rev.* **52** 295

Wilmore D and Hodgson P E 1964 *Nucl. Phys.* **55** 673